

# 3

## Computational Industrial Mechanics Programme (CIMP)

*Sophisticated mathematical modelling aided by powerful computing and visualization has the potential to provide the cutting-edge to industry; generation of cost-effective solutions, process optimization and product design are some of the areas where modelling and simulation can play critical to enabling role. The C-MMACS Computational Industrial Mechanics Programme (CIMP) seeks to develop and apply tools of mathematical modelling and computer simulation in diverse areas of engineering.*

### ***Highlights***

*The Year 2005-06 for CIMP is characterized by development and refinement of a number of theoretical and conceptual issues in the areas of finite element analysis, elastodynamics, numerical algorithms and non-linear dynamics.*

### ***Inside***

- *Static and Free Vibration Analysis of 6-noded Triangle Element under Mesh Distortion*
- *The Unsymmetric Finite Element Formulation and Variational Incorrectness*
- *Effect of Inertia on the Dynamics of a Periodically Forced Spherical Particle in a Quiescent Fluid*

### 3.1 Static and Free Vibration Analysis of 6-noded Triangle Element under Mesh Distortion

The classical Lagrangian finite elements will perform poorly under a distorted mesh. Distorted meshes can slow down the convergence of the solutions and may give inaccurate results. The distorted meshes are unavoidable when we do the analysis of complex structures. The distortion sensitivity of the elements is not completely studied in available literatures. A 2-D element can have an angular distortion or a mid-node distortion. The angular distortion will appear in meshes with curved geometries, transition region from coarse mesh to fine mesh and the nonlinear problems with large deformations. Fracture mechanics problems will lead to mid node distortion. To address the 2-D effects of mesh distortion, the 6-noded triangular element with plane stress conditions had been considered. The quadratic displacement is assumed to derive the metric shape functions so that the completeness condition has been satisfied. Depending on the shape function used, the elements are classified into parametric (PP), metric (MM), parametric-metric (PM) and metric-parametric elements (MP). An in-house finite element code had been developed in MATLAB platform to compute the displacements/stresses for the static analysis and to compute the natural frequencies for the free vibration analysis of structural mechanics problems with and without mesh distortion.

Static analysis is carried to assess the behaviour of the proposed PP, MM, PM and MP elements. Two

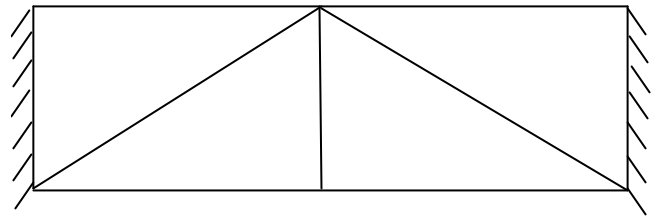


Figure-3.1a - without distortion

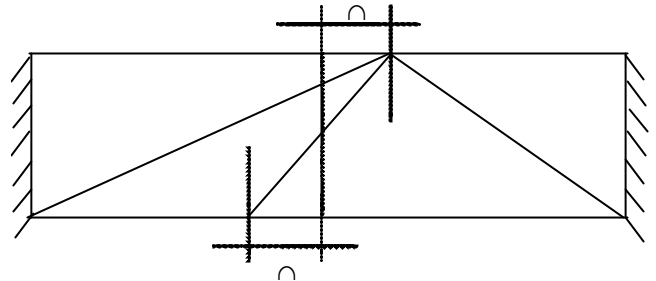


Figure-3.1b - with distortion

types of problems are analyzed, namely a cantilever beam with tip moment and a cantilever beam with a tip shear force under various types of mesh distortions. The numerical test results prove that when there is distortion, only the PM formulation behaved better than the classical finite element. A fixed-fixed bar behaviour had been simulated using 6-noded element for repeated image and mirror image with distortion (Figure 3.1a & 3.1b). This problem had been considered for the free vibration analysis. From the numerical test, it had been seen that the PM element gives more accurate natural frequencies than the conventional PP element. Interestingly, the MP element results are identical with PM element results of the various types of mesh distortions for the free vibration analysis and it will

Table 3.1 First natural frequencies of fixed - fixed bar of 6-noded elements with repeated image

Delta	Exact	PP	PM	MM	MP
0.125	9.86960440	10.91826588	9.97362492	9.93573539	9.97362492
0.100	9.86960440	10.47162887	9.95262833	9.93543675	9.95262833
0.075	9.86960440	10.20699465	9.93723811	9.93076495	9.93723811
0.050	9.86960440	10.04118839	9.92689163	9.92506193	9.92689163
0.000	9.86960440	9.91907349	9.91907349	9.91907349	9.91907349
-0.050	9.86960440	10.04118839	9.92689163	9.92506193	9.92689163
-0.075	9.86960440	10.20699465	9.93723811	9.93076495	9.93723811
-0.100	9.86960440	10.47162887	9.95262833	9.93543675	9.95262833
-0.125	9.86960440	10.91826588	9.97362492	9.93573538	9.97362492

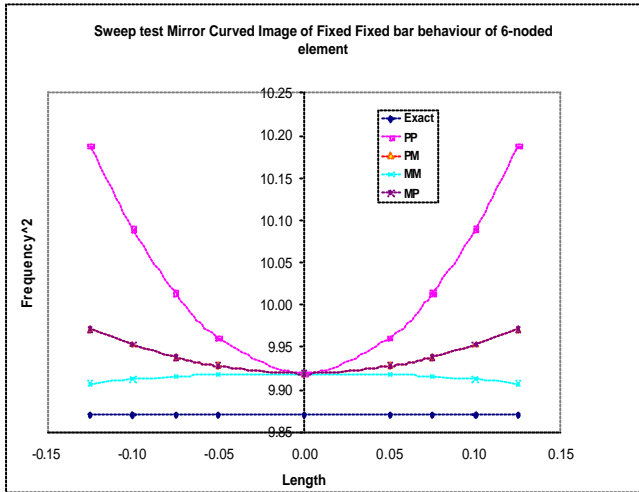


Figure-3.2 Sweep test for 6-noded element with fixed-fixed bar behaviour.

be valid for all the cases with different boundary conditions under admissible distorted geometry shapes. But the MP element behaves poorly in static analysis. Distortion parameter  $\delta$  had been varied to understand the elements behaviour and the natural frequencies are listed in Table-3.1. Also sweep test had been performed to analyze distortion sensitivity for the mirror image element (Figure-3.2).

V Senthilkumar and G Prathap

### 3.2 The Unsymmetric Finite Element Formulation and Variational Incorrectness

The unsymmetric finite element formulation has been proposed recently to improve predictions from distorted finite elements. We examine here whether the unsymmetric formulation is variationally correct. From the weak form in terms of the energy inner product for the exact solution, we ensure that the

symmetric formulations, namely the PP and MM versions are both variationally correct, and produce best-fit results. The PM formulation, even though it is practically a very useful device to meet the continuity requirements and the best-fit stress recovery requirements in a distorted element, is not variationally correct. A fixed-fixed bar with single element of an axial load at mid span had been analyzed. Table 3.4 displays the results from a single-element mesh using the PM and MM models described above of the test case when the distortion term  $\zeta$  is varied. Immediately, we notice that the displacements  $u_3$  from the two FEM models, and for whatever value of distortion, are exact! However, this is not true of the displacement  $u_2$  for all the cases displayed in Table 3.2.

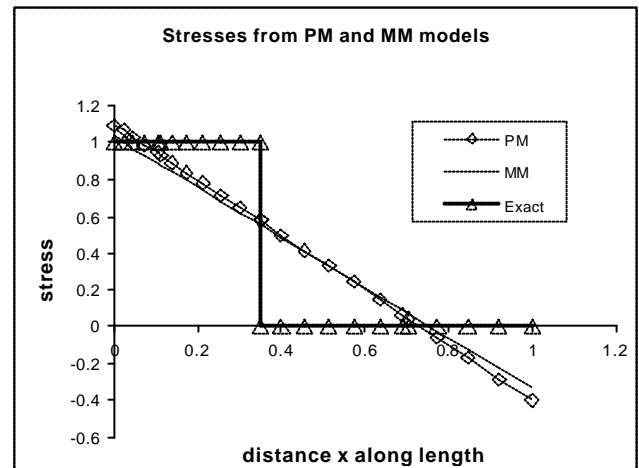


Figure 3.3 Stresses from PM and MM models compared with exact stress when concentrated load is placed at  $x_2 = 0.35$

Figure 3.3 shows the variation of stresses computed from the displacements from the PM and MM models as compared to the exact stress in the bar when the concentrated load is placed at  $x_2 = 0.35$  ( $\zeta = -0.15$ ). Both PM and MM, due to the use of the M-trial

Table 3.2 Displacements  $u_2$  and  $u_3$  for a single-element test of fixed-free bar with concentrated load of  $P = 1$  at node  $N_2$  as location  $x_2$  is moved by  $\zeta$ .

Disp.	$\zeta = 0$			$\zeta = -0.05$			$\zeta = -0.15$		
	MM	PM	Exact	MM	PM	Exact	MM	PM	Exact
$u_2$	0.4375	0.4375	0.500	0.3863	0.3881	0.450	0.2778	0.2931	0.350
$u_3$	0.500	0.500	0.500	0.450	0.450	0.450	0.350	0.350	0.350

functions, give a linear variation. It can be very easily checked that the stress from MM (shown by the thin solid line) is an exact best-fit of the actual stress variation (thick solid line) whereas the stress from PM (thin broken line) is in error. The geometric

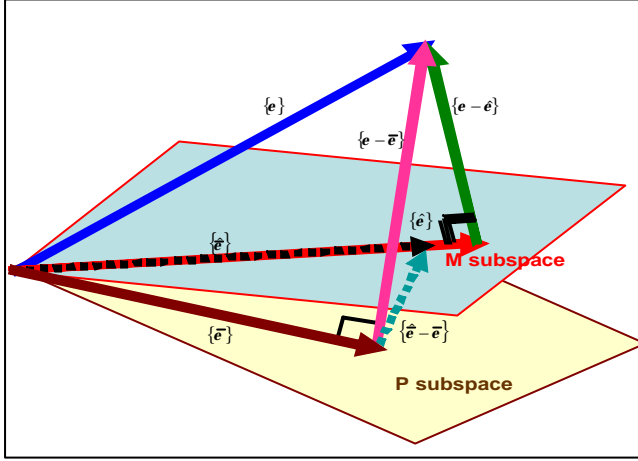


Figure 3.4 The geometric representation of the PP, MM and the PM finite element computation from the best-fit and the function space point of view.

representation of the PP, MM and the PM finite element computation from the best-fit and the function space point of view is shown in Figure 3.4.

When it comes to a distorted mesh, especially in 2D and 3D modelling, one has to choose between satisfying the continuity condition on the edges of adjoining element and the variational correctness of the correspondence between the actual stress and the approximate stress. We could also succeed in using the best-fit paradigm to predict independently from first principles, the stresses that the unsymmetric PM formulation will produce in an actual finite element computation. The PM formulation is not an exact best-fit of the exact solution  $u$  and we are concluding that the stress from the PM formulation will be orthogonal to the stress from the PP formulation. This is seen in Figure 3.4.

*G Prathap , S Manju , V Senthilkumar  
and P Jafarali*

### 3.3 Effect of inertia on the Dynamics of a Periodically Forced Spherical Particle in a Quiescent Fluid

We have formulated the problem using the formalism of Lovalenti and Brady (1993) for the problem of the

motion of a periodically forced spherical particle in a quiescent fluid at low Reynolds Numbers. The formalism of Lovalenti and Brady (1993) for the case of the motion of a spherical particle in a fluid at low Reynolds Numbers is:

$$\begin{aligned}
 F^H(t) = & \frac{4\mathbf{p}}{3} \text{Re } S I U^x(t) - 6\mathbf{p} U_s(t) - \frac{2\mathbf{p}}{3} \text{Re } S I U_s(t) \\
 & + \frac{3}{8} \left( \frac{\text{Re } S I}{\mathbf{p}} \right)^{\frac{1}{2}} \left\{ \int_{-\infty}^t \left[ \begin{aligned} & \frac{2}{3} F_s^{H_{\parallel}}(t) - \left\{ \frac{1}{|A|^2} \left( \frac{\mathbf{p}^{\frac{1}{2}}}{2|A|} \text{erf}(|A|^2) - \exp(-|A|^2) \right) \right\} F_s^{H_{\parallel}}(s) \right. \\ & \left. + \frac{2}{3} F_s^{H_{\perp}}(t) - \left\{ \exp(-|A|^2) - \frac{1}{2|A|^2} \left( \frac{\mathbf{p}^{\frac{1}{2}}}{2|A|} \text{erf}(|A|) - \exp(-|A|^2) \right) \right\} F_s^{H_{\perp}}(s) \right] \frac{2ds}{(t-s)^{\frac{3}{2}}} \right\} + 0(\text{Re}) \quad (1)
 \end{aligned}
 \right.
 \end{aligned}$$

The various terms in this equation are defined in the original paper of Lovalenti and Brady (1993). We note here that this formalism yields the hydrodynamic force acting on a spherical particle moving with a certain time dependent velocity in a Newtonian fluid which is moving with an arbitrary time dependent

uniform velocity. We have used this formalism to develop the equation for the motion of a periodically forced sphere in a quiescent fluid. We note certain features of this equation which need to be kept in mind when we develop numerical solutions to our equation. First we note that the equation is nonlinear

and contains an improper integral which has to be evaluated taking all past values of both the instantaneous position and velocity of the particle. The equation is nonlinear because the variable 'A' in the formalism of Lovalenti and Brady (1993) is a function of both the current value of the position of the particle and its past value. We also note that there is a singularity in the integral which is not bounded at 's', the past time equal to 't', the current time. This singularity has to be treated appropriately in order to evaluate the integral at each time step when we perform a numerical integration of the equation of motion. We checked that our interpretation of the improper integral was reasonable by reproducing a known result, namely, Figure 5 of Lovalenti and Brady (1993).

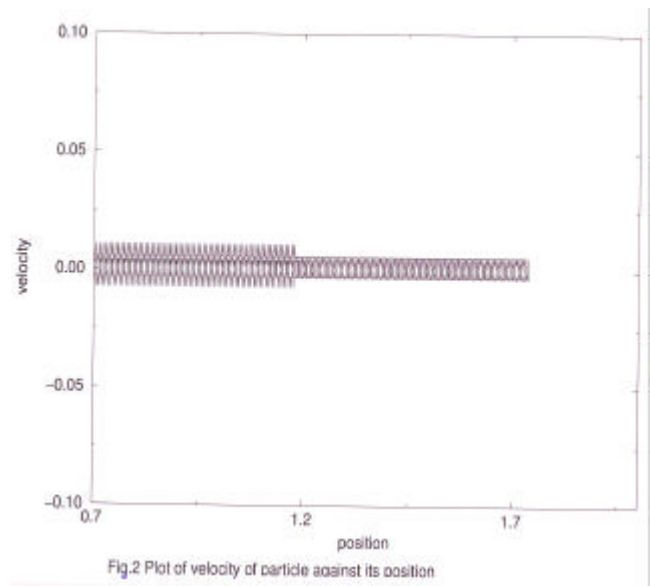
The equations for a periodically forced spherical particle in a quiescent fluid, as derived, from the formalism of Lovalenti and Brady (1993) are :

$$\begin{aligned} \frac{dY_p}{dt} &= U_p \\ \frac{dU_p}{dt} &= \frac{6\mathbf{p}}{\text{Re}St} \text{Sin}(t) - \frac{6\mathbf{p}U_p}{\text{Re}St} \left\{ \left( \frac{\text{Re}Sl}{\mathbf{p}} \right)^{\frac{1}{2}} \frac{1}{2} \int_0^t \frac{ds}{(t-s)^{\frac{3}{2}}} + 1 \right\} \\ &+ \frac{9}{2} \left( \frac{\text{Re}Sl\mathbf{p}}{\text{Re}St} \right)^{\frac{1}{2}} \int_0^t \left\{ \frac{1}{A^2} \left( \frac{\mathbf{p}^{\frac{1}{2}}}{2A} \text{erf}(A) \right) - e^{-A^2} \right\} \left[ \frac{U_p(s)}{(t-s)^{\frac{3}{2}}} \right] ds \end{aligned} \quad (2)$$

We note that this is a system of two coupled nonlinear non-autonomous equations. In these equations,  $Y_p$  is the position of the particle,  $U_p$  is the velocity of the particle,  $\text{Re}$  is the Reynolds Number,  $\text{Sl}$  is the Strouhal Number,  $\text{Re}St$  is defined as  $4/3 \text{Re} + 2/3 \text{Re}Sl$  and is a small positive number;  $A$  is defined in terms of the position of the particle at the current time and the position at a past time, 's' as;

$$A = \frac{\text{Re}}{2} \frac{(t-s)^{\frac{1}{2}}}{(\text{Re}Sl)^{\frac{1}{2}}} \left( \frac{Y_p(t) - Y_p(s)}{t-s} \right) \quad (3)$$

We note that velocities are scaled with respect to the product of the size of the spherical particle and the frequency of the periodic force; position is scaled with respect to the size of the spherical particle and time, 't', is scaled with respect to the frequency of the external force field; force is scaled with respect to the product of the size of the particle, the viscosity of the fluid phase and the characteristic velocity. The definitions for  $\text{Re}$  and  $\text{Sl}$  then follow from the scaling as mentioned above; 's' is the past time scaled with reference to the frequency of the driving force.



When we solved the equation of motion for a selected set of parameters, we noticed certain features of the solution. We observed that the solution for the velocity oscillated about a small positive value. This implied that the position of the spherical particle varied slowly with time. This feature of there being a small non-zero drift velocity of the spherical particle may be considered similar to the presence of a small non-zero drift force in the case of a fluctuating suspension of colloidal spheres as shown by Hinch and Nitsche (1993) upon the inclusion of inertial effects. This is shown in Figure 3.5 for a typical value of the parameters. The value of the small positive velocity around which the velocity of the particle oscillated was a function of the parameters and generally decreased with the value of  $\text{Re}$ . A qualitative explanation of this behavior may be obtained by averaging the equation of motion over a period of the driving force. Upon averaging the equation of motion, we obtain:

$$\frac{d\bar{U}_p}{dt} = \frac{-6\mathbf{p}\bar{U}_p}{\text{Re}St} \left\{ 1 + \left( \frac{\text{Re}Sl}{\mathbf{p}} \right)^{\frac{1}{2}} \left( \frac{1}{\mathbf{e}} \right)^{\frac{1}{2}} \right\} + \frac{6\mathbf{p}}{\text{Re}St} \int_0^{2p} \frac{U_p(s)}{s^{\frac{1}{2}}} ds$$

$$+ \frac{3}{2} \frac{\text{Re}\mathbf{p}^{\frac{1}{2}}}{\text{Re}St} \bar{U}_p^2 + \frac{9}{2} \frac{(\text{Re}Sl\mathbf{p})^{\frac{1}{2}}}{\text{Re}St} \int_0^{2p} \left( \int_0^{t-e} ds \right) dt \quad (4)$$

When we set the left hand side of the equation to zero indicating that the average velocity changes very slowly with time we see from the above equation that it admits a positive value of the average velocity in addition to the zero average velocity. A more physical explanation might be that the inclusion of inertia which automatically excludes fore-aft symmetry in the flow field around the spherical particle might lead to a small residual positive value of the average velocity. We also note another striking feature of the solutions, namely that there is a qualitative change in the behaviour of the solution

at around 500 time units. This might represent the time taken for the flow field induced by the oscillation of the particle to reach an approximate steady state. The resulting plot of the position of the particle with scaled time shows a small change in slope at this time and the phase space plot of the velocity of the particle with the position of the particle shows a sharp reduction in the amplitude of the velocity oscillations. There are some solutions in the literature for the force induced by an oscillatory motion of a spherical particle. However the presence of the non-linearity in our equation makes it difficult to compare our results with those results. Further most of the literature which deals with inertial effects considers the force due to a given imposed velocity of the sphere. Our situation where we consider the effect of a periodic force on the motion of a small spherical particle has received considerably less or no attention to our knowledge.

***T R Ramamohan***